International Journal on Engineering Technology and Infrastructure Development (InJET-InDev)
www.lec.edu.np/journal
Volume 2, Issue no. 1, Page 132-142
Received Date: 9/26/2024
Revised Date: 6/27/2025
Accepted Date: 6/28/2025
ISSN: 3021-999X (Print)

Structural Performance of the RC T-Girder Superstructure of Gongabu Bridge under Vehicular Loads

Bini Neupane[1]
[1]*Department of Civil Engineering, Kathmandu University, Dhulikhel, Kavre, Nepal, neupanebini123@gmail.com*

Abstract

This research focuses on the structural assessment of a reinforced concrete T-girder bridge located near Gongabu Buspark in Kathmandu, which spans the Bishnumati River. The bridge was selected for analysis due to its age, visible signs of deterioration, and its role in supporting daily urban traffic. Linear Static Analysis and Moving Load Analysis was carried out in CSI Bridge version 20.2.0 for serviceability, structural strength and equilibrium load combinations given in IRC 6:2017. The deflections, forces and stresses for linear static and moving load analysis were obtained and checked for the permissible values. The analyses revealed that the deflection during the moving load analysis exceeded the maximum permissible limit, which may be a contributing factor to the longitudinal cracks observed during visual inspection. However, other factors such as aging of concrete, environmental effects, and inadequate maintenance may also have played a significant role in the deterioration.

Keywords: Moving Load Analysis, Bridge, Structural Deflection, Non-Destructive Testing, Retrofitting

1. Introduction

Bridges play a crucial role in transportation networks by enabling people and goods to cross natural barriers like rivers, valleys, and roads. Reinforced concrete (RC) bridges are especially popular because they offer a good balance of strength, durability, and cost-effectiveness. Despite heavy investments worldwide in road infrastructure, bridges remain some of the most vulnerable parts due to factors like design mistakes, aging, corrosion, and inadequate maintenance. These issues can seriously affect their safety and performance over time.

Several international studies highlight the importance of regular bridge monitoring and upkeep. For example, (Figueiredo, et al., 2022) pointed out that bridge failures can have serious social and economic consequences. Their research stressed the value of modern technologies, such as smartphone-based systems, to improve early detection of damage in bridges. Similarly in 2021, (Ambroziak & Malinowski, 2021) studied a 95-year-old concrete arch bridge in Jagodnik, Poland. They used material tests and computer simulations to evaluate the bridge's condition and emphasized that fixing old bridges requires close cooperation between engineers and researchers. Together, these studies show a growing global focus on using data and new technology to manage bridge safety proactively.

In Nepal, many of the challenges seen internationally are also present. According to the Department of Roads, there are currently 2,022 bridges nationwide, with 1,658 on National Highways. Kathmandu Valley alone has 50 bridges totaling 2,289 meters in length. Many of these, especially those along the East-West Mahendra Highway, have been in use for more than 50 years longer than their original design life. Most were built with outdated materials and standards, raising concerns about their ability to handle today's traffic safely. To address these issues, this research focused on Kathmandu Valley, where several aging RC bridges were inspected and tested. A T-girder bridge over the Bishnumati River near Gongabu Buspark was selected for detailed study through numerical modeling and non-destructive testing.

Recent studies in Nepal have helped improve understanding and management of the country's bridges. (Pant & Shrestha, 2022) introduced a quality index for bridge decks based on non-destructive tests like Ultrasonic Pulse Velocity (UPV) and rebound hammer methods. These allow engineers to find cracks and voids inside concrete

without harming the structure. Likewise, (Lama, et al., 2022) assessed the Bagmati Bridge using sensor monitoring and finite element analysis. Their research showed how combining physical inspections with dynamic testing can reveal early signs of damage, especially in the superstructure.

This research begins with a visual inspection, which is a key initial step in assessing the condition of bridges. Visual inspection involves a careful and systematic examination of all visible parts of the bridge, such as girders, decks, joints, and supports, to identify any obvious signs of damage like cracks, corrosion, or deformation. During this process, inspectors documented and measured any defects they observe using tools such as crack gauges and tape measures, and they recorded detailed notes and photographs. This method helped to provide an overall understanding of the bridge's current physical state.

The visual inspection of the RC T-girder bridge at Gongabu Ringroad over the Bishnumati River allowed for the identification of critical areas that required further investigation. Based on these findings, non-destructive tests, including rebound hammer tests to assess concrete strength and rebar locator surveys to identify reinforcement positions, were conducted to gather more precise data without damaging the structure. This combination of visual and non-destructive inspections formed the basis for developing structural drawings and models.

Following the inspection phase, the structural behavior of the bridge was analyzed using two main approaches: linear static analysis and moving load analysis, both performed with CSI Bridge version 20.2.0 software. This software was chosen because it is designed specifically for bridge engineering and offers practical tools to model complex bridge structures accurately. It can simulate real-life load conditions, like moving traffic, which are important to understand how the bridge behaves under actual use. The program is easy to use and has features that make the analysis of bridges faster and more efficient.

When using CSI Bridge, certain assumptions were made to simplify the analysis. For example, materials were considered homogeneous and isotropic, and the bridge components were modeled with idealized connections and boundary conditions. These simplifications allowed for efficient calculations while still capturing the main behavior of the structure, although some local effects or nonlinear material responses were not fully represented.

These analyses helped to understand how the bridge responded to different loading conditions and revealed any weaknesses in the structure. Visual inspection was therefore essential in this research because it provided the necessary real condition data that guided testing and modeling efforts.

2. Methodology

This research involved conducting linear static analysis and moving load analysis on the RC T-Girder bridge located at Gongabu Ring Road over the Bishnumati River. The purpose was to understand how the bridge responds to various load combinations. The process began with a visual inspection and measurement of different bridge components. Non-destructive tests, such as rebound hammer and rebar locator assessments, were also performed. These tests helped in preparing detailed drawings of the bridge. Finally, the structural model of the bridge was developed using CSI Bridge version 20.2.0, which was then used to perform various analyses.

2.1. Visual Inspection of Gongabu Ring Road Bridge:

The Gongabu Ringroad Bridge exhibited several structural problems during the visual inspection, as shown in Figure 1. Longitudinal cracks were visible along the bridge deck, which are likely due to weaknesses at the construction joints. These joints often act as points of stress concentration, especially when proper construction practices are not followed. Over time, the continuous impact of heavy traffic loads has made these cracks more severe. Furthermore, signs of scouring were noticed around the pier and pile foundation. Scouring, often caused by flowing water removing soil from around the foundation, can lead to loss of support and increased vulnerability of the structure. These findings indicate that the bridge's structural condition has been affected by both age and environmental factors. The general features of the bridge are provided in Table 1.

Figure 1. Gongabu Ringroad Bridge

Table 1. General Features of Gongabu Ringroad Bridge [Source: Department of Roads]

Length	65 m
Span Length=	Span_1=16.6m, Span_2=16m, Span_3=16m, Span_4=16.4m
Number of Span=	4
Abutment Type	Stone Masonry
Abutment Foundation	Open Foundation
Pier Type	RCC
Pier Foundation	Pile Foundation
Super Structure	RCC T- Beam
Bearings	Steel Bearing
Construction Year	1977
Age	47 years

After the visual inspection of all these bridges, Gongabu Ringroad bridge was taken into consideration for the further analysis.

2.2. Non-Destructive Test:

The following tests were carried out to evaluate the properties of concrete and locate the reinforcements:

i. Rebound Hammer Test

The Rebound Hammer Test was performed in accordance with (IS13311(Part2), 1992) to estimate the surface hardness and in-situ compressive strength of concrete in key structural elements of the bridge. The test was conducted on the main girder, cross girder, deck slab, pier head, and pier using a Schmidt Rebound Hammer in a horizontal orientation as shown in Figure 2.

Before testing, all surfaces were cleaned to remove dust, laitance, and loosely adhered particles to ensure accuracy. The testing was carried out using a grid spacing of 25 mm between points, with each impact point kept at least 20 mm away from edges or any surface discontinuities as per standard requirements. At each grid location, multiple

rebound readings were recorded. For each structural component, 20 readings were taken, and to improve result reliability, the five highest and five lowest values were excluded. The mean of the remaining 10 readings was then used to estimate the compressive strength.

Based on the recorded rebound numbers and corresponding standard conversion charts for the Schmidt Hammer Model N/NR, the estimated compressive strengths of the components were as follows and also shown in Table 2: Main Girder: 20 MPa, Cross Girder: 25 MPa, Pier Head: 40 MPa, Pier: 30 MPa and Deck Slab: 35 MPa.

These values provide an indicative assessment of the concrete's condition in each structural member. While the results give a useful data of surface-level strength, it should be noted that rebound hammer values are influenced by several factors, including surface moisture, concrete age, and carbonation. Additionally, this method assesses strength only to a limited surface depth and may not detect internal micro-cracks or flaws. According to the standard, the probable accuracy of the estimated strength is ±25%. Therefore, these results are best interpreted as preliminary indicators and should ideally be supplemented with core tests or other detailed evaluation methods for conclusive assessment.

Figure 2. Rebound Hammer Test

Table 2. Results of Rebound Hammer Test

COMPONENTS OF BRIDGE	**COMPRESSIVE STRENGTH(Mpa)**
MAIN GIRDER	20
CROSS GIRDER	25
PIER HEAD	40
PIER	30
SLAB	35

ii. Rebar Locator Test:

The Rebar Locator was used to detect the position and layout of reinforcing bars within different parts of the bridge, such as the main girder, cross girder, pier, and slab. The device was carefully moved across the surface first from left to right, and then from bottom to top to identify the embedded steel reinforcement without damaging the concrete as shown in Figure 3. This helped in marking the location of the bars accurately.

The main purpose of the test was to locate the rebar arrangement so that detailed drawings could be prepared and any future drilling or retrofitting work could be planned safely. The use of the Rebar Locator made it possible to understand the internal reinforcement pattern, which is essential for structural analysis and design verification.

However, it is important to mention that the test did not measure the tensile strength of the reinforcement bars. The equipment used in this study was limited to locating the bars only. To determine the actual tensile strength,

destructive tests such as sample extraction and laboratory tensile testing would be required. This was not part of the current research scope.

Figure 3. Locating and marking spacing of rebar in main girder

2.3. Preparation of Detailed Drawing of the Bridge:

Since there were no available as-built drawings of the bridge, detailed plans were developed using data from the Rebar Locator Test and the minimum requirements from the IRC Guidelines. The reinforcement for each bridge component was determined based on this information. The detailed drawings, including the plan, transverse section, longitudinal section, and reinforcement details of all components, were created using AutoCAD.

Figures 4 through 8 illustrate the following: the plan and elevation of the bridge (Figure 4), the transverse section of the bridge (Figure 5), and the reinforcement details of the main girder (Figure 6), cross girder (Figure 7), and pier (Figure 8), with all dimensions provided in meters.

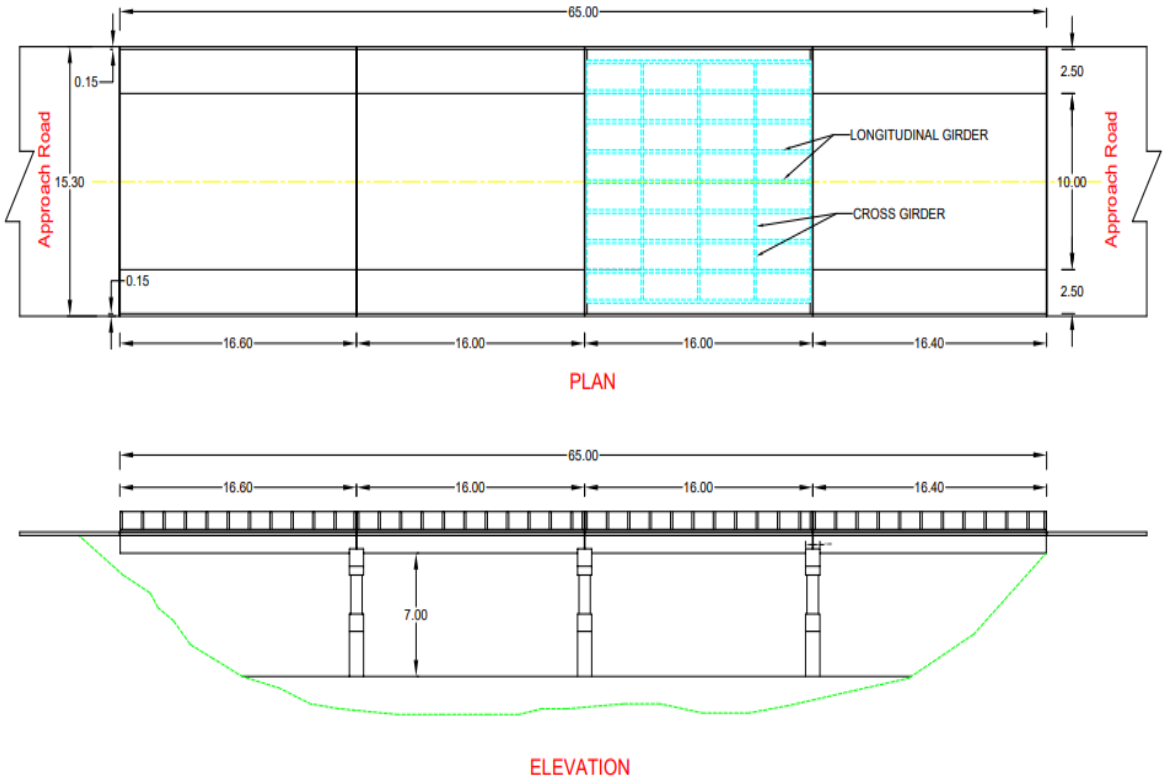

Figure 4. Plan and Elevation of bridge

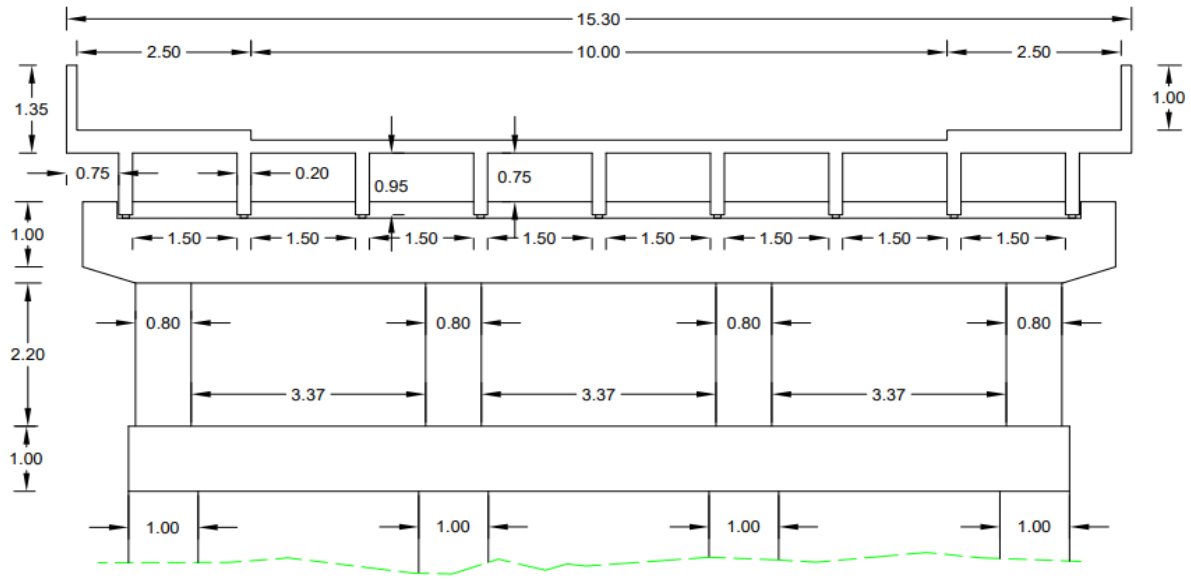

Figure 5. Transverse Section of the Bridge

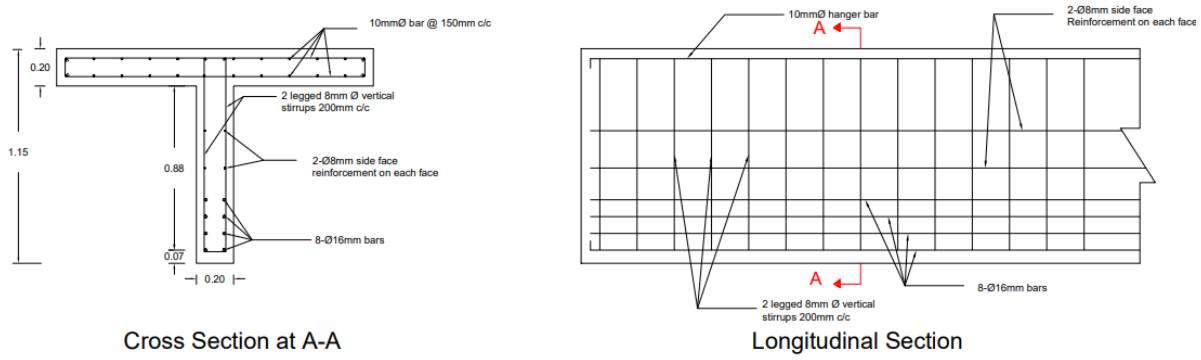

REINFORCEMENT DETAILS OF MAIN GIRDER

Figure 6. Reinforcement Details of Main Girder (All dimensions are in meters)

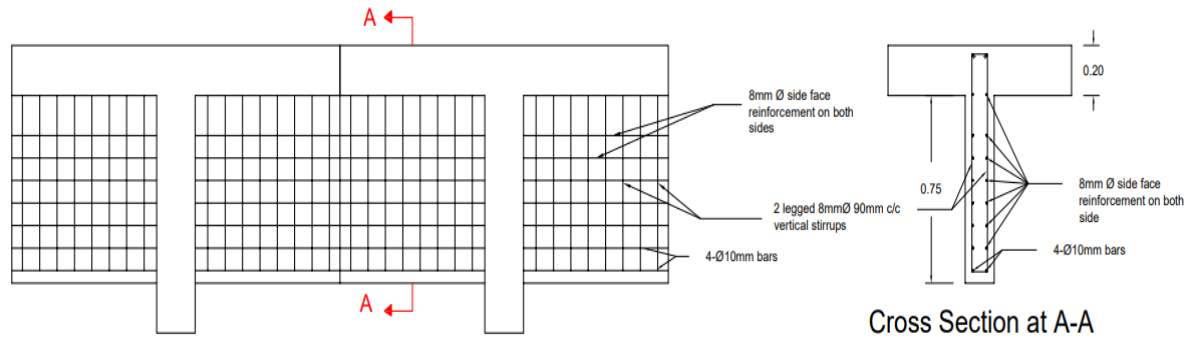

REINFORCEMENT DETAILS OF CROSS GIRDER

Figure 7. Reinforcement Details of Cross Girder (All dimensions are in meters)

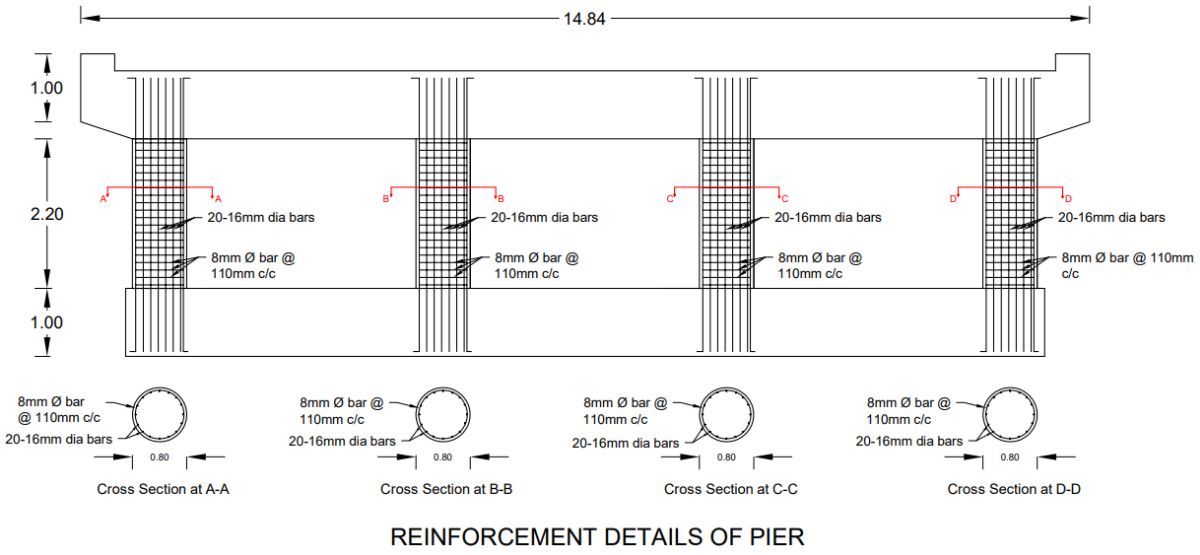

Figure 8. Reinforcement Details of Pier (All dimensions are in meters)

2.4. Development of Structural Model in CSI Bridge:

The structural model of the bridge was developed using CSI Bridge v20.2.0, following the standards of (IRC:6-2017). The bridge consists of four simply supported spans measuring 16.60 m, 16.00 m, 16.00 m, and 16.40 m respectively, giving a total span length of 65.00 m. The carriageway width is 10.00 m, with additional 2.50 m wide footpaths on both sides, making the total width 15.30 m as shown in the bridge plan.

The modeling process involved defining layout and reference lines, assigning section and material properties, and incorporating realistic support conditions and boundary restraints. The following assumptions and modeling principles were adopted for different components of the bridge:

i. Deck slab was modeled as a shell element with isotropic concrete material properties assigned according to M20 grade concrete, assuming uniform thickness.

ii. Longitudinal and cross girders were modeled as frame elements, with the reinforcement not modeled separately but accounted for through effective section stiffness.

iii. Piers were modeled as fixed-base vertical frame elements, assuming rigidity at the base (pile connection) and linear elastic behavior.

iv. Pier foundations (piles) were not explicitly modeled in 3D due to data limitations, but were simulated using fixed supports to approximate pile-soil interaction.

v. Bearings were represented as pinned connections with translational restraint in vertical direction and rotational freedom, based on standard steel bearing behavior assumptions.

The material properties used in the model were based on Rebound Hammer test for concrete and Fe 415 steel, assuming original design strength. Due to the absence of time-dependent degradation models or long-term monitoring data, material aging effects were not incorporated. This is recognized as a limitation of the study.

In terms of traffic lane configuration, the carriageway width of 10.00 meters was modeled as a two-lane system, following the lane width recommendations of IRC:6-2017, which suggests 3.5 to 3.75 meters per lane for highways. Each lane was defined as 3.75 meters wide, with the remaining space considered as a buffer or shoulder.

Although the 2.50 m wide footpaths on either side are physically present on the bridge, they were not modeled as separate traffic lanes. Instead, their load contribution was included as a uniformly distributed load in the load definition phase. The absence of separate footpath lane modeling is noted as a limitation, which may slightly affect load path and stiffness distribution in pedestrian scenarios.

As shown in Table 3, the loads applied to the bridge included 3 KN/m for railings, 9.375 KN/m for the sidewalk, 1.5 KN/m for pedestrians, and 2 KN/m2 for asphalt. Load combinations, as per (IRC:6-2017), are provided in Table 4.

In this study, various vehicle loading classes were considered during the structural analysis of the bridge, in line with the provisions of (IRC:6-2017). The code specifies standard loading configurations to represent different types of traffic commonly observed on national highways. Since the bridge is located on the Gongabu Ringroad in Kathmandu, which carries both light and heavy vehicles, multiple loading classes were applied to realistically simulate traffic conditions and evaluate the bridge's performance.

The loading classes used in the analysis included IRC Class A, Class AA (tracked and wheeled), and IRC 70R (tracked and wheeled). IRC Class A represents typical highway traffic and is the standard loading requirement for all permanent bridges. It was used as a baseline in this study. Class AA loading was included to account for occasional heavier traffic, such as military or industrial vehicles. Both the tracked and wheeled forms of Class AA were modeled. The tracked version represents vehicles like tanks or machinery, while the wheeled version simulates multi-axle commercial vehicles.

IRC 70R loading, which includes both tracked and wheeled variants, was also considered. This is the heaviest category of vehicle loading defined in the IRC code, used for bridges expected to carry exceptionally heavy loads such as military convoys or large commercial transport vehicles. Although the bridge spans are moderate in length, using 70R loading ensures the structure is evaluated under extreme conditions, particularly important for a major urban route like the Ringroad.

In the CSI Bridge model, these vehicle classes were applied using their respective axle loads, spacings, and configurations as defined in (IRC:6-2017). The model included two traffic lanes, each 5.0 meters wide, corresponding to the total 10-meter carriageway. In addition, the bridge has 2.5-meter-wide footpaths on both sides, bringing the total transverse width of the structure to 15.3 meters. While the footpaths were not modeled as separate lanes, their effect was considered by applying a uniformly distributed load across their areas.

Vehicle movements were simulated as moving loads across the lanes to generate the structural response under different traffic scenarios.

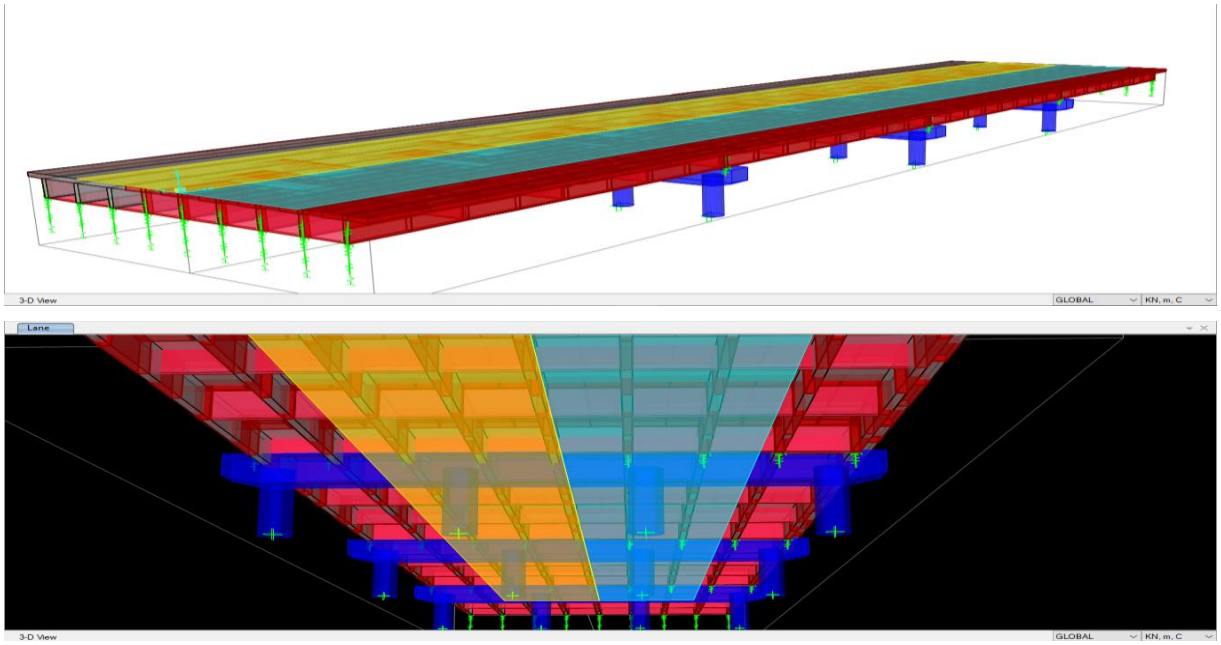

Figure 9. 3D view of the Bridge

Table 3. Load Defined for bridge

RAILING	3 KN/m
SIDEWALK	9.375 KN/m
PEDESTRIAN	1.5 KN/m

Asphalt	2 KN/m2	

Table 4. Load Combination as per (IRC:6-2017)

STRUCTURAL STRENGTH	1.75Asphalt+1.35DL+1.5VL+1.5PL+1.35Railings+1.35Sidewalks	(IRC:6-2017), Table B.2
SERVICEABILITY LIMIT STATE	1.2Asphalt+1.0DL+1.0VL+1.0PL+1.0Railings+1.0Sidewalks	(IRC:6-2017), Table B.3
EQUILIBRIUM	1.35Asphalt+1.1DL+1.5VL+1.5PL+1.1Railing+1.1Sidewalks	(IRC:6-2017), Table B.1

3. Result and Discussion

The structural response of the bridge under various load combinations was analyzed using CSI Bridge. Table 5 presents the maximum vertical deflection values observed in each span under different loading scenarios, while Figures 10 and 11 illustrate the deflected shapes and critical regions. Among all spans, span 4 exhibited the highest deflection of 17.434 mm under moving load analysis. This was compared against the allowable serviceability limit for live load deflection.

While (IRC:6-2017) does not specify explicit limits for vertical deflection, the ((AASHTO), 2002) recommend a conservative deflection limit of L/1000 for live loads to ensure user comfort and structural serviceability. For a span of 16.6 meters, this translates to a maximum allowable deflection of 16.6 mm. The observed value of 17.434 mm in Span 4 exceeds this limit, indicating potential serviceability concerns under moving vehicle loads.

Under dead load only, the maximum deflection recorded was 23.623 mm in Span 4, which remains well within the typical design limit of L/250 (approximately 66.4 mm). However, it's important to note that serviceability deflection checks are generally intended for live load-only conditions, not dead load alone. Therefore, the critical observation remains the live load (moving load) deflection exceeding the AASHTO L/1000 criterion.

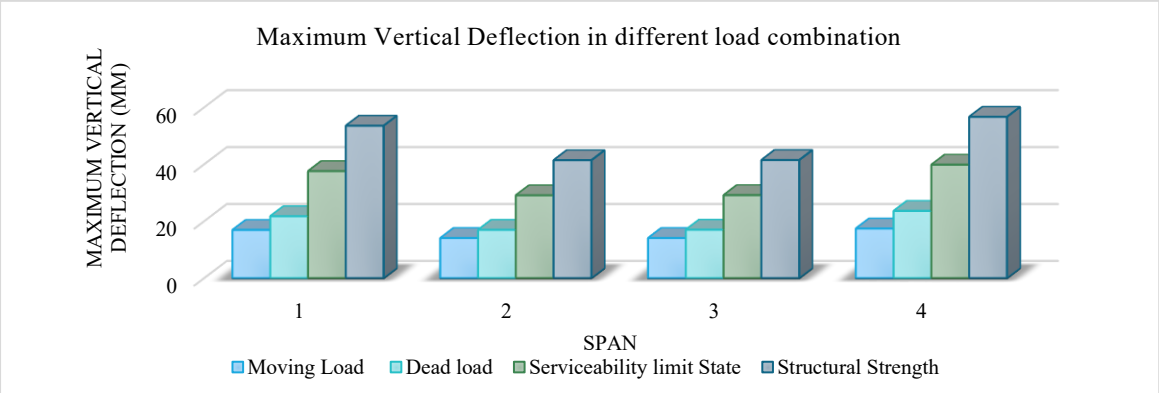

Figure 10. Maximum Vertical Deflection for different Load Combination

Table 5. Maximum Vertical Deflection

LOAD/SPAN	**Maximum Vertical Deflection (mm)**			
	Span 1	**Span2**	**Span3**	**Span4**
Moving Load	16.94	14.087	14.093	17.434
Dead load	21.744	16.966	17.015	23.623
Serviceability limit State	37.61	29.11	29.16	39.86
Structural Strength	53.55	41.43	41.5	56.67

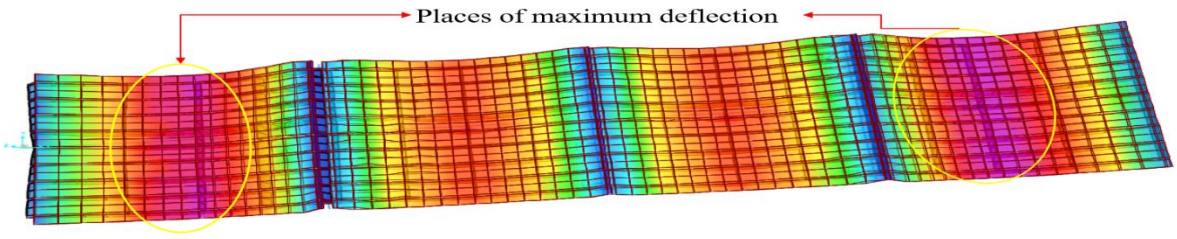

Figure 11. Places for maximum for moving load case

The tensile stress observed in the bottom fiber of the bridge girder during analysis reached a value of 22.11 MPa. To verify whether this could be resisted by the concrete, an estimate of the material's flexural tensile strength was made based on (IS456:2000), Clause 6.2.2, which recommends the following empirical formula:

$f_r = 0.7\sqrt{f_{ck}}$=3.13 MPa, this calculation shows that M20 concrete can resist up to approximately 3.13 MPa in flexural tension, which is far below the 22.11 MPa observed in the numerical analysis. This implies that the observed tensile stress is being resisted primarily by the steel reinforcement, not the concrete. If such stresses occur in unreinforced or poorly bonded sections, they could contribute to surface cracking.

Indeed, longitudinal cracks observed during visual inspection, especially in Span 1 and Span 4, correspond with the locations of high deflection and stress concentration. These findings suggest that the bridge is experiencing more strain under vehicle loading than originally designed for, likely due to both increased traffic loads and material aging. It's important to note that while moving loads were considered in the analysis, no explicit dynamic (impact or vibration) loading was modeled.

Based on these observations, it is recommended that targeted retrofitting measures be applied, particularly in Span 4, to reduce deflection and extend service life. Solutions such as externally bonded FRP, steel plate strengthening, or prestressing may be explored. It is also advised to install a Structural Health Monitoring (SHM) system to monitor deflections, crack propagation, and load behavior over time. Lastly, a traffic load reassessment is needed to determine whether current vehicle demands exceed the bridge's original design capacity, and whether future upgrades or replacement should be considered.

Acknowledgements

I would like to express my sincere gratitude to the Department of Civil Engineering, Kathmandu University, for their invaluable guidance and support throughout this research. I am also deeply thankful to ACME Technotrade Concern (P) Ltd. for providing the necessary resources and technical assistance that made this study possible.

References

(AASHTO), A. A. o. S. H. a. T. O., 2002. *AASHTO LRFD Bridge Design Specifications.* Washington, D.C.: s.n.

1992, I. 1. (. 2., n.d. *Non- Destructive Testing of Concrete- Methods of Test, Part2: Rebound Hammer.* s.l.:Bureau of Indian Standards.

Ambroziak, A. & Malinowski, M., 2021. A 95-Year-Old Concrete Arch Bridge: From Materials Charaterization to Structural Analysis. *materials.*

Department of Roads, B. B., n.d. Department of Roads.

Falyo, D. & Holland, B., 2017. *Medical and psychosocial aspects of chronic illness and disability.* s.l., s.n.

Figueiredo, E. et al., 2022. Smartphone Application for Structural Health Monitoring of Bridges. *Sensors.*

IRC:6-2017, Seventh Revision. *SECTION: II LOADS AND LOAD COMBINATIONS,* s.l.: s.n.

IS13311(Part2), 1992. *non-destructive testing of concrete methods of test, part 2: rebound hammer,* s.l.: s.n.

IS456:2000, 2000. Plain and Reinforced Concrete – Code of Practice (Fourth Revision). In: s.l.:s.n.

Lama, M., Mandal, B. & Tamang, M., 2022. Structural Health Assessment of the Bagmati Bridge. *Proceedings of 12th IOE Graduate Conference,* October.pp. 1030-1034.

lee, s. & kalos, n., 2015. bridge inspection practices using non-destructive. *journal of civil engineering and management,* 21(5)(issn 1392-3730 / eissn 1822-3605), pp. 654-665.

Pant, U. & Shrestha, J. K., 2022. Bridge Deck Quality Indexing based on Non-Destructive Tests. *Proceedings of 12th IOE Graduate Conference,* October, Volume 12, pp. 352-357.

Rehman, S. K. U., Ibrahim, Z., Memon, S. A. & Jameel, M., 2016. Nondestructivetestmethodsforconcretebridges:Areview. *ConstructionandBuildingMaterials,* pp. 58-86.

Roads, D. o., n.d. *Department of Roads, Bridge Branch.* [Online]
Available at: https://dor.gov.np/bridgebranch

Skyler, J. et al., 2017. *Differentiation of diabetes by pathophysiology, natural history, and prognosis.* s.l., s.n.

Xu, D., Xu, X., Forde, M. C. & Caballero, A., 2023. Concrete and steel bridge Structural Health Monitoring-Insight into choices for machine learning applications. *Construction and Building Materials.*